J. Fluid Mech. (2012), *vol.* 706, *pp.* 34–45. © Cambridge University Press 2012
doi:10.1017/jfm.2012.176

The universal aspect ratio of vortices in rotating stratified flows: experiments and observations

Oriane Aubert[1]†, Michael Le Bars[1], Patrice Le Gal[1] and Philip S. Marcus[2]

[1] Institut de Recherche sur les Phénomènes Hors Equilibre, UMR 7342, CNRS and Aix-Marseille Université, 49 rue F. Joliot Curie, 13384 Marseille, CEDEX 13, France

[2] Department of Mechanical Engineering, University of California, Berkeley, CA 94720, USA

(Received 19 January 2012; revised 28 February 2012; accepted 1 April 2012;
first published online 25 May 2012)

We validate a new law for the aspect ratio $\alpha = H/L$ of vortices in a rotating, stratified flow, where H and L are the vertical half-height and horizontal length scale of the vortices. The aspect ratio depends not only on the Coriolis parameter f and buoyancy (or Brunt–Väisälä) frequency $\bar{N}$ of the background flow, but also on the buoyancy frequency N_c within the vortex and on the Rossby number Ro of the vortex, such that $\alpha = f\,[Ro(1+Ro)/(N_c^2 - \bar{N}^2)]^{1/2}$. This law for α is obeyed precisely by the exact equilibrium solution of the inviscid Boussinesq equations that we show to be a useful model of our laboratory vortices. The law is valid for both cyclones and anticyclones. Our anticyclones are generated by injecting fluid into a rotating tank filled with linearly stratified salt water. In one set of experiments, the vortices viscously decay while obeying our law for α, which decreases over time. In a second set of experiments, the vortices are sustained by a slow continuous injection. They evolve more slowly and have larger $|Ro|$ while still obeying our law for α. The law for α is not only validated by our experiments, but is also shown to be consistent with observations of the aspect ratios of Atlantic meddies and Jupiter's Great Red Spot and Oval BA. The relationship for α is derived and examined numerically in a companion paper by Hassanzadeh, Marcus & Le Gal (*J. Fluid Mech.*, vol. 706, 2012, pp. 46–57).

Key words: rotating flows, stratified flows, vortex flows

1. Introduction: vortices in stratified rotating flows

The Great Red Spot (GRS) and other large vortices such as the Oval BA (Marcus 1993) are persistent giant anticyclonic vortices in Jupiter's atmosphere. Their vertical aspect ratios $\alpha = H/L$ lie in the range $0.03 \leqslant \alpha \leqslant 0.1$. In the Atlantic Ocean, meddies are also long-lived anticyclones made of water of Mediterranean origin that is warmer and saltier than the ambient Atlantic. Their lifetimes can be as long as several years, and they have $\alpha \simeq 0.01$ (with $H \simeq 0.5$ km and $L \simeq 50$ km). Presumably, the aspect ratios of these vortices are the result of a competition between rotation and stratification. A rapidly rotating flow, parameterized by a large Coriolis parameter f and small characteristic azimuthal velocity V_θ (i.e. small Rossby number $Ro = V_\theta/fL$)

† Email address for correspondence: aubert@irphe.univ-mrs.fr

is controlled by the Taylor–Proudman theorem: flows have little variation along the rotation axis and form columnar vortices with large α. In contrast, strongly stratified flows, parameterized by large buoyancy frequencies

$$N \equiv \sqrt{-\frac{g}{\rho}\frac{\mathrm{d}\rho}{\mathrm{d}z}} \tag{1.1}$$

inhibit vertical motions and form baroclinic vortices, often appearing as thin 'pancake' vortices (Billant & Chomaz 2001). Here ρ is the fluid density, g is gravity and z is the vertical coordinate.

The goal of this paper is to investigate this competition and determine and verify a quantitative law for α. Previous experimental studies that used constant-density fluids to simulate Jovian vortices (Antipov *et al.* 1986; Sommeria, Meyers & Swinney 1988) prohibited this competition and resulted in laboratory vortices that were barotropic Taylor columns that extended from the bottom to the top of the tank. Thus, α was imposed by the boundaries of the tank. In our experiments, the vortices are created near the centre of a large tank so that the tank's boundaries have no or little influence on α and there is little or no Ekman circulation in the tank and no Ekman spin-down of our vortices.

2. Aspect ratio law of a model vortex

The dissipationless, Boussinesq equations for a fluid with mean density ρ_0 in the rotating frame (and ignoring the centrifugal force) are

$$\left.\begin{aligned}\frac{\partial \boldsymbol{v}}{\partial t} &= -(\boldsymbol{v}\cdot\boldsymbol{\nabla})\boldsymbol{v} - \frac{\boldsymbol{\nabla} p}{\rho_0} + f\boldsymbol{v}\times\hat{\boldsymbol{z}} - \frac{(\rho-\rho_0)}{\rho_0}g\hat{\boldsymbol{z}}\\ \frac{\partial \rho}{\partial t} &= -(\boldsymbol{v}\cdot\boldsymbol{\nabla})(\rho-\bar{\rho}) + v_z\,\rho_0\,\frac{\bar{N}^2}{g}\end{aligned}\right\} \tag{2.1}$$

where $\boldsymbol{v}$ is the divergence-free velocity, v_z the vertical component of the velocity, p is the pressure, z is the vertical coordinate, $\hat{\boldsymbol{z}}$ is a unit vector and an overbar above a quantity indicates that the quantity is the equilibrium value in the undisturbed, linearly stratified (i.e. with constant $\bar{N}$) fluid. The unperturbed solution has $\bar{\boldsymbol{v}} = 0$; $\bar{\rho} = -(\bar{N}^2/g)\rho_0 z + \rho_0$; and $\bar{p} = (\bar{N}^2\rho_0/2)\,z^2 - g\,\rho_0\,z + p_0$, where p_0 is an arbitrary constant. One steady solution of the Boussinesq equations that consists of an isolated, compact vortex with solid-body rotation Ω has $\boldsymbol{v} \equiv \bar{\boldsymbol{v}} = 0$, $\rho \equiv \bar{\rho}$ and $p \equiv \bar{p}$ everywhere outside the vortex boundary, while inside the vortex we have $v_\theta = \Omega\, r$, $v_z = v_r = 0$, $\rho = -(N_c{}^2/g)\,\rho_0\,z + \rho_0$ and

$$p = (N_c{}^2\,\rho_0/2)\,z^2 - g\,\rho_0\,z + [\Omega\,(\Omega + f)\,\rho_0/2]\,r^2 + p_c \tag{2.2}$$

where r is the cylindrical radial coordinate, v_r and v_θ are the radial and azimuthal components of the velocity; p_c is a constant equal to $p_0 - \rho_0\,\Omega\,(\Omega + f)\,L^2/2$, and L is the radius of the vortex at $z = 0$. This vortex has a uniform buoyancy frequency N_c throughout the entire vortex (in general, the subscript c means that the quantity is to be evaluated at the vortex centre, i.e. at $r = 0$ and $z = 0$). The vortex boundary is determined by requiring the pressure to be continuous throughout the flow. Note that the density and velocity are discontinuous at the vortex boundary. Continuity of p requires the vortex boundary to be ellipsoidal:

$$(r/L)^2 + (z/H)^2 = 1, \tag{2.3}$$

where the semi-height is $H \equiv \sqrt{2\,(p_0 - p_c)/[\rho_0\,({N_c}^2 - \bar{N}^2)]}$, and the semi-diameter is $L \equiv \sqrt{2\,(p_0 - p_c)/[\Omega\,\rho_0\,(f + \Omega)]}$. The aspect ratio of this vortex is

$$\alpha \equiv H/L = \left(\frac{Ro\,(1 + Ro)}{{N_c}^2 - \bar{N}^2}\right)^{1/2} f, \tag{2.4}$$

where the Rossby number $Ro \equiv \omega_c/2f = \Omega/f$. We have defined Ro in terms of the vertical vorticity ω at the vortex centre to make our expression in (2.4) consistent with a more general relationship for α that is derived in the companion paper by Hassanzadeh, Marcus & Le Gal (2012) by assuming that the vortex has cyclo-geostrophic balance in the horizontal directions and hydrostatic balance in the vertical direction. One can see that the law requires for cyclones in equilibrium to have $Ro > 0$, $p_0 > p_c$ and $N_c > \bar{N}$; for cyclostrophic anticyclones in equilibrium, the law requires $Ro < -1$, $p_0 > p_c$ and $N_c > \bar{N}$, but for quasi-geostrophic anticyclones it requires $-1 < Ro < 0$, $p_0 < p_c$ and $N_c < \bar{N}$.

3. Comparison with previous observations or predictions of vortex aspect ratio α

Our law (2.4) for the aspect ratio α agrees with previous experiments in rotating and stratified flows. For example, Bush & Woods (1999) created vortices in a rotating stratified fluid from the break-up of small-diameter rising plumes. In these experiments, very little ambient fluid becomes entrained in a rising plume or when the plume breaks and rolls up into vortices, so the vortex cores have nearly uniform density ($N_c = 0$). Owing to angular momentum conservation, the fluid within plumes rising from a small diameter orifice have no angular momentum or angular velocity when viewed in the inertial frame. When viewed in the rotating frame with angular velocity $f/2$, these plumes have an angular velocity $\Omega = -f/2$. Thus, in the rotating frame these vortices are anticyclones with $Ro \simeq -0.5$. With parameter values $N_c = 0$ and $Ro = -0.5$, (2.4) predicts $\alpha = 0.5f/\bar{N}$, which agrees well with the experiments of Bush & Woods (1999) that found $\alpha = 0.47f/\bar{N}$.

It is often claimed that quasi-geostrophic (QG) vortices obey the scaling law $H/L = f/\bar{N}$ (McWilliams 1985; Dritschel, de la Torre Juarez & Ambaum 1999; Reinaud, Dritschel & Koudella 2003), independently of the values of Ro and N_c. This scaling is broadly used among the oceanographic community for vortices created from noise but is sometimes applied to Atlantic meddies and other vortices without close neighbours. We show in §§ 4 and 5 that the aspect ratios of our experimental vortices and meddies have shapes that strongly depend on Ro and their internal stratifications N_c, and therefore $\alpha \neq f/\bar{N}$ for these vortices.

In a theoretical, inviscid analysis, Gill (1981) analytically computed a solution for a two-dimensional vortex (that is, a unidirectional zonal flow, in contrast to an axisymmetric vortex). He found an interior solution of the zonal flow and an exterior solution to that flow and then matched them together requiring that the density and all components of the velocity were continuous at the interface between the two solutions, which are the appropriate conditions for a flow with dissipation. He found that the exterior flow had an aspect ratio α proportional to $Ro(f/\bar{N})$. We believe that Gill's analysis is flawed because he imposed too many matching conditions for a dissipationless flow, where only the normal component of the velocity is continuous (see our model in § 2). It can be shown that with the proper matching conditions the aspect ratio of Gills zonal flow is equal to our scaling law for α in (2.4) in the geostrophic limit where $Ro(1 + Ro) \to Ro$ (see Hassanzadeh *et al.* 2012). Hedstrom &

Armi (1988) experimentally tested the scaling law derived by Gill. Based on our own experiments that attempted to reproduce those of Hedstrom & Armi (1988), it appears that the measurements they carried out were made while the vortices were very young, still undergoing geostrophic adjustment and far from equilibrium.

Note finally that our law, modified for use with discrete layers of fluid rather than a continuous stratification, also applies to the models of anticyclonic ocean eddies used by Nof (1981) and by Carton (2001).

4. Application to laboratory vortices

We have carried out a study of vortices in a rotating, stratified laboratory flow in a transparent tank of dimensions 50 cm × 50 cm × 70 cm mounted on a rotating table. Using the classic double-bucket method with salt water (Oster 1965), each experiment initially has a linear vertical stratification, with a constant buoyancy frequency $\bar{N}$ independent of location. The values of $\bar{N}$ in our experiments varied from 1 to 2.3 rad s^{-1}. The Coriolis parameter f can be as large as 7 rad s^{-1}. Two sets of experiments were carried out following works by Griffiths & Linden (1981) and Hedstrom & Armi (1988). In the first set, once the fluid in the tank reaches solid-body rotation, we briefly inject a small volume of fluid with constant density ρ_0 through a 2.5 mm diameter pipe along the axis of rotation at depth approximately midway between the top and bottom of the tank. As soon as the fluid is injected, it is deflected horizontally by the stratification and the Coriolis force organizes it into a freely decaying anticyclone. In the second set of experiments, the vortex is permanently sustained by a smooth and stationary injection, using a peristaltic pump whose flux rate is chosen between 6 and 500 mL min^{-1}, through the 2.5 mm diameter pipe with a sphere of porous material fixed at the end of the pipe. The technique in the second set of experiments allows us to create vortices with higher Rossby numbers than in the first set. Moreover, the sustained anticyclones in the second set of experiments evolve very slowly compared with those in the first set. In both sets of experiments, the injected fluid is seeded with fluorescein dye and 100 μm – diameter particles for particle image velocimetry (PIV) (Meunier & Leweke 2003). We follow the evolution of the vortices using one horizontally and one vertically illuminated laser sheet. Video images of the vertical cross-section allow us to record the changes in time of the vortex aspect ratio (figure 1*a,b*), while the PIV measurements in the horizontal sheet allow us to find the azimuthal and radial components of the velocity of the vortex, which lead to the determination of *Ro* (figure 1*c,d*).

4.1. *Freely decaying vortices*

The brief injection of fluid with density ρ_0 at height z_0 (where $\bar{\rho}(z_0) \equiv \rho_0$) is immediately followed by fast adjustments where the injected fluid becomes approximately axisymmetric. After axisymmetrization, $|V_\theta|$ and $|Ro|$ decay very slowly in time with the vortices persisting for 1000–1800 table rotation times ($4\pi/f$), or several hundred turnaround times of the vortices ($2\pi/(fRo)$). During the slow decay, the vortex core passes through a series of quasi-equilibrium states where it has approximately solid-body rotation with negligible radial velocity as shown in figure 1(*d*). The experimentally measured boundaries of one of the slowly decaying anticyclones that were created by injection are shown at four different times in figure 2. Also shown are the boundaries of our theoretical model of the decaying vortex. Our model is the solid-body rotating vortex with a discontinuous velocity derived in § 2 with $N_c \equiv 0$ and with the ellipsoidally shaped boundary given by (2.3).

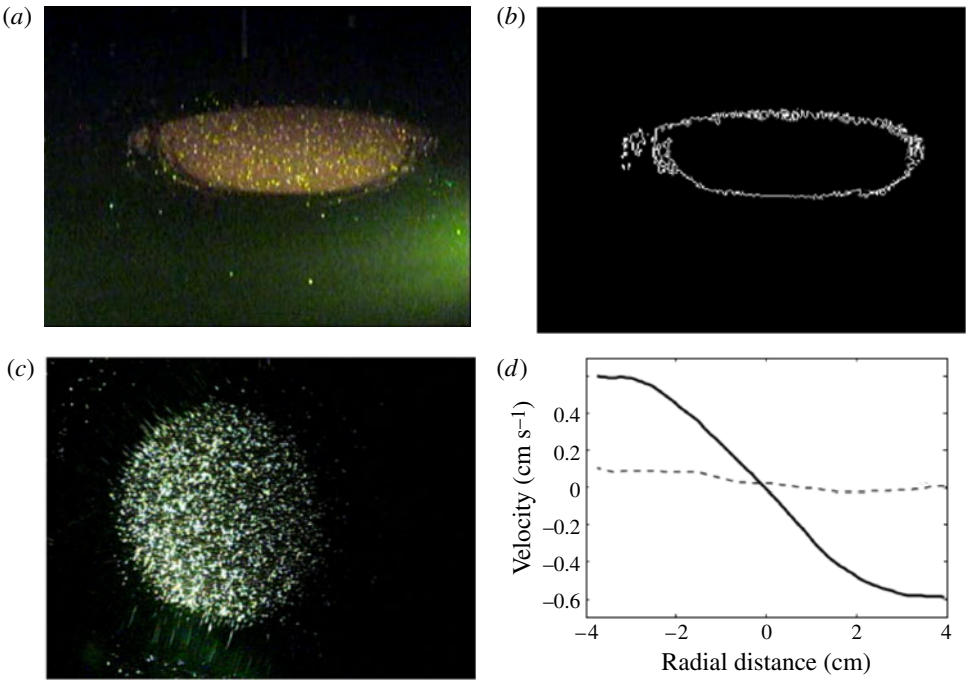

FIGURE 1. (Colour online available at journals.cambridge.org/flm) Aspect ratio and Rossby number. (*a,b*) Determination of the aspect ratio $\alpha = H/L$. (*a*) Side view of a laboratory anticyclone with $\bar{N} = 2.3$ rad s^{-1} and $f = 2$ rad s^{-1}. (*b*) Image processing of vortex in (*a*) to determine α. Here $\alpha = 0.3$ with $H = 1.9$ cm and $L = 6.3$ cm. (*c,d*) Determination of Ro. (*c*) Top view of laboratory anticyclone with $\bar{N} = 2$ rad s^{-1}, $f = 2$ rad s^{-1}, and $Ro = -0.13$. (*d*) Azimuthal v_θ (−) and radial v_r (− −) velocities of flow in (*c*) as functions of radius r. The core has a solid-body-like rotation. The magnitude of v_r is consistent with the r.m.s. fractional uncertainty of v_θ, which is ±5–10 %. The fractional uncertainties in $\bar{N}$ are ±10 %.

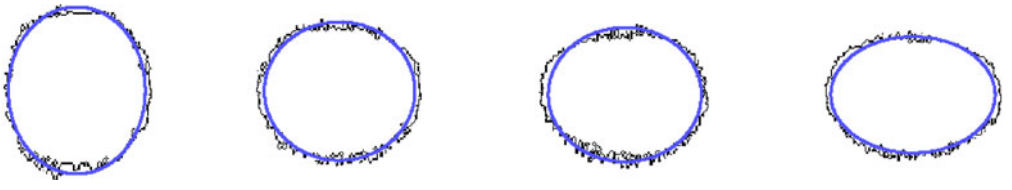

FIGURE 2. (Colour online) Image-processed side view of a vortex boundary (black) at different times t with $f = 6.8$ rad s^{-1} and $\bar{N} = 1.6$ rad s^{-1} held fixed. Here $|Ro|$ decreases in time. Also shown are the theoretical boundaries (grey in print; blue online) of the model vortices at each time. The model vortex has H/L given by (2.4), so the coincidence of the grey (or blue) and black curves validates our law. Here $T = 4\pi/f$ is the period of the rotating turntable. Because $f/\bar{N} = 4.25$ is the same for all of these vortices, while α differs, it is clear that the scaling law $\alpha = f/\bar{N}$ is not correct for these vortices.

Owing to the slow diffusion of salt, we assume that for all time the fluid density within the model vortex remains at its initial value of ρ_0, so we assume that $N_c = 0$ for all time. Owing to the lack of diffusion in the laboratory vortex, we also assume that within the ellipsoidal boundary of the model vortex, the volume $4/3\pi H(t)L(t)^2 = 4/3\pi\alpha(t)L(t)^3$ remains constant, despite the fact that α and L change in time. The theoretical boundaries of our model vortices are computed with (2.3), where $\alpha(t)$ is given by our law (2.4), where $Ro(t)$ is measured experimentally, N_c is assumed to be zero, f is known, $\bar{N}$ is assumed to remain at its initial value and where $L(t)$ is computed by assuming that the volume of the ellipsoid is constant in time. That is, we set

$$L(t) = L_0\ [\alpha_0/\alpha(t)]^{1/3} \tag{4.1}$$

where the value of L_0 is the experimental value of L from the first panel with $Ro = -0.08$; α_0 is the initial value of α found from (2.4) with $Ro = -0.08$ and $\alpha(t)$ is determined from $Ro(t)$ using (2.4).

Figure 2 shows that the boundaries of the laboratory and model vortices are nearly coincident at four different times, and at those times the vortices have four different Rossby numbers and four different aspect ratios. This validates the law (2.4) for α and also shows that our assumptions that $N_c = 0$ and that the volume of the vortex remains constant are both good. If the correct scaling law were $H/L = f/\bar{N}$ rather than law (2.4), then the vortex in figure 2 would have the same aspect ratio through time, which it clearly does not. Using the scaling law of Gill (1981) with a Ro dependence would lead to a smaller predicted aspect ratio by a factor between 3.4 and 6.

4.2. *Vortices sustained by continuous injection*

In the second set of experiments, the vortices are sustained by a continuous injection of fluid with density ρ_0 at a fixed flux rate, as in the experiments of Griffiths & Linden (1981). The characteristic values of Ro for these vortices range between -0.45 and -0.20. The volume of the vortices slowly increases in time and Ro decays very slowly compared with the viscously decaying vortices discussed in § 4.1. The continuous injection is laminar and the rate of injection is sufficiently small so that the volume of the vortices increases by only approximately 1 % per table rotation. As a consequence, we use the same theoretical, elliptical model that we used for the viscously dissipating vortices analysed in § 2. The experimentally measured boundaries at four different times of a vortex sustained with continuous injection are shown in figure 3. As before, the aspect ratio of the extracted shape of the laboratory vortex is compared with α of our model vortex from law (2.4) with $N_c = 0$, the observed value of Ro, and the volume calculated with the flux rate of the experiment and time t/T. As can be seen, the comparison is excellent and validates our theoretical law (2.4) in the cyclo-geostrophic regime.

Note that in the similar experiments of Griffiths & Linden (1981), briefly described in section 5 of their article, continuous injections into a linearly stratified fluid were performed. They observed vortices with aspect ratios of 0.47 and 0.99. In these two experimental runs, $\bar{N}H/fL$ was estimated around 0.3, which is in disagreement with QG law $N/L = f/\bar{N}$. As no precise measurement of Ro was done, no comparison is possible with either our law or Gill's theory (Gill 1981).

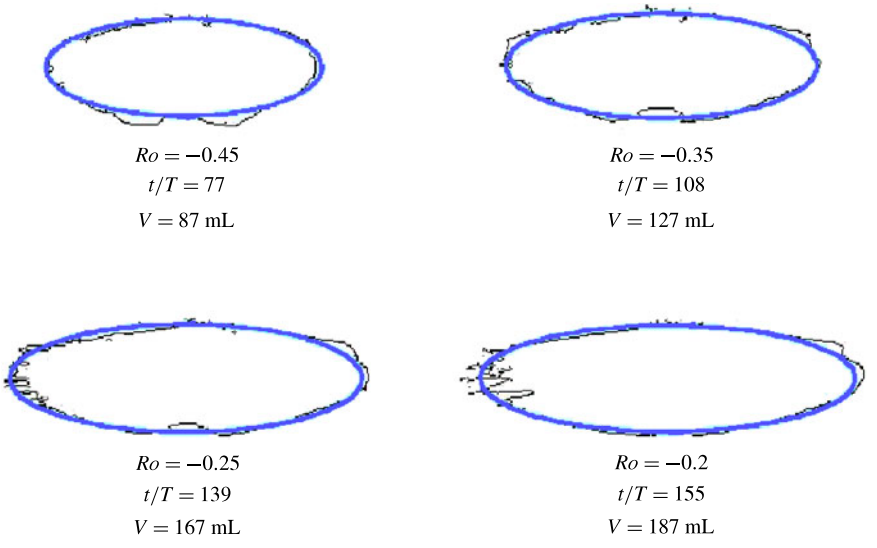

FIGURE 3. (Colour online) Image-processed side-view boundaries of a vortex sustained with continuous injection at different times. The flow has $f = 1.62$ rad s^{-1}, $\bar{N} = 2.3$ rad s^{-1} and an injection rate of 10 mL min^{-1}. Also shown are the theoretical boundaries of the model vortices. Line colours are as in figure 2. The model vortex has H/L given by (2.4), so the coincidence of the boundaries of the laboratory and model vortex validates (2.4) for α. Unlike the vortex in figure 2, the vortex volume V changes in time. Here Ro, V and time t are given for each image.

5. Application to meddies and Jovian vortices

Our law (2.4) for vortex aspect ratio α also applies to ocean meddies, which, unlike our laboratory vortices, are internally stratified (i.e. $N_c \neq 0$). Using the reported values of the ocean densities as functions of position within and outside the meddies (Armi *et al.* 1988; Hebert, Oakley & Ruddick 1990; Pingree & Le Cann 1993; Tychensky & Carton 1998), we have compiled in table 1 average values of the buoyancy frequencies of the meddies N_c and their background environments $\bar{N}$, along with the observed values of α, L and Ro. Note that according to our relationship (2.4) for the aspect ratio, the effects of non-zero N_c do matter on the aspect ratio, especially when N_c is of order $\bar{N}$, as it is for the meddies (and Jovian vortices; see below). For all but the oldest meddy shown in figure 4, law (2.4) fits the observations. Note that setting α equal to the alternative scaling $f/\bar{N}$ does not fit the meddy data, even with the large uncertainties of the observed values of α of the meddies shown in figure 4. Setting α equal to the other alternative scaling discussed in § 3, $Ro\,(f/\bar{N})$ (Gill 1981; Hedstrom & Armi 1988), is an even poorer fit.

Law (2.4) also applies to Jovian vortices. For the GRS it is necessary to take into account the fact that the characteristic horizontal length L of the derivative of the pressure anomaly $(p - \bar{p})$ is nearly three times smaller than the characteristic radius R_v where the azimuthal velocity reaches its peak value (Shetty & Marcus 2010). As shown in our companion paper by Hassanzadeh *et al.* (2012), when $R_v > L$, the law should be modified so that $Ro\,(1 + Ro)$ in (2.4) is replaced with $Ro\,[1 + Ro\,(L/R_v)]$. With the exceptions of H and N_c, the properties of Jovian vortices are well known and have small uncertainties (Shetty & Marcus 2010).

https://doi.org/10.1017/jfm.2012.176 Published online by Cambridge University Press

Data	$\sqrt{\bar{N}^2 - N_c^2}$ (rad s^{-1})	N_c (rad s^{-1})	f (rad s^{-1})	*Ro*	*Observed* α	L (km)
Experiment 1	1.6	0	6.8	−0.32 to −0.02	1.71 to 0.68	—
Experiment 2	1.6	0	3.2	−0.16 to −0.03	0.82 to 0.38	—
Experiment 3	2.3	0	1.6	−0.45 to −0.2	0.36 to 0.27	—
Bush and Wood's experiment	0.78 to 1.4	0	0.4 to 2.2	−0.5	0.13 to 1.32	—
Meddy Ceres	0.0022	0.002	8.46×10^{-5}	−0.05	0.0073	35
Meddy Hyperion	0.0024	0.0018	8.46×10^{-5}	−0.07	0.009	45
Meddy Encelade	0.0026	0.0015	8.1×10^{-5}	−0.08	0.009	45
Meddy Sharon	0.0021	0.0011	7.7×10^{-5}	−0.15	0.01	32
Meddy Bobby	0.0015	0.0017	8.3×10^{-5}	−0.17	0.018	27
Jupiter's Oval BA	0.0048	0.018	1.92×10^{-4}	−0.16	0.014	3200
Jupiter's GRS	0.0047	0.015	1.37×10^{-4}	−0.38	0.020	2300 ($R_V = 6260$ km)

TABLE 1. Data for figure 3. The three sets of laboratory experiments listed in the top three lines have different values of $\bar{N}$ and f. Experiment 1 and 2 correspond to freely decaying vortices and experiment 3 to a sustained vortex. Each set of experiments had vortices with different values of *Ro*, but in all of our laboratory experiments, we assumed $N_c = 0$ and $R_v = L$. Here $2L$ and $2H$ were defined to be the horizontal and vertical diameters of the vortices as determined by our edge-finding algorithm (cf. figure 1). The uncertainties in the laboratory measurements are dominated by the small non-axisymmetric component of the vortices. The fractional uncertainties in $\bar{N}$ are $\pm 10\,\%$. For the meddies, the values of $\bar{N}$ and N_c are such that $1.33 < \bar{N}/N_c < 2.16$. The parameter values and their uncertainties for the Jovian vortices are discussed in § 5 and in the online supplementary material. Note that the Jovian values of $\bar{N}$, f and L are known with small uncertainties but that H has large uncertainties.

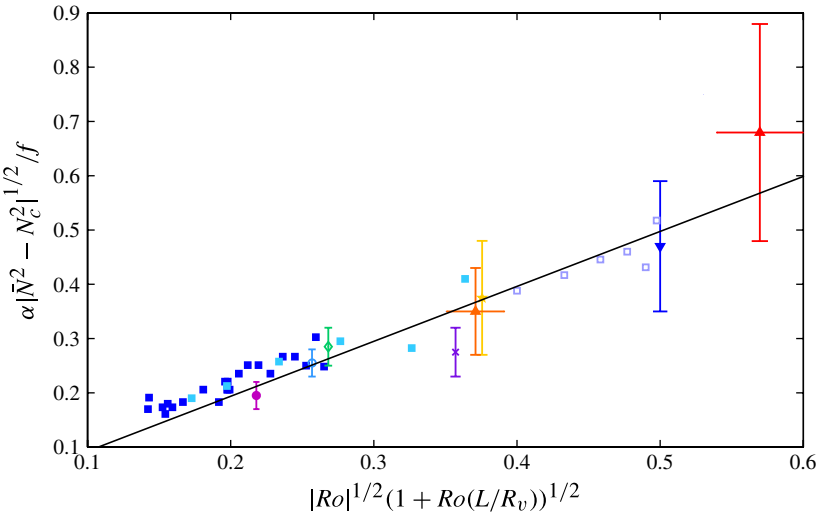

FIGURE 4. (Colour online) Tests of our theoretical law (2.4) (straight line) for α. The theory agrees with our freely decaying vortex experiments (■) with $1.6\ \mathrm{rad\ s^{-1}} \leqslant f \leqslant 7\ \mathrm{rad\ s^{-1}}$ and with our sustained vortex experiments with $f = 1.6\ \mathrm{rad\ s^{-1}}$ and $N = 2.3\ \mathrm{rad\ s^{-1}}$(□); with Bush and Woods' experiments at $Ro = -0.5$ (Bush & Woods 1999) (▼); with Jupiter's GRS and Oval BA (Marcus 1993; de Pater *et al.* 2010; Shetty & Marcus 2010) (▲); and with meddies Sharon (Armi *et al.* 1988; Hebert *et al.* 1990; Schlutz Tokos & Rossby 1990) (×), Bobby (Pingree & Le Cann 1993) (⋆), Hyperion (○), Ceres (●) and Encelade (◇) (Tychensky & Carton 1998). All of the data for the meddies are given in table 1. Data and error bars for the Jovian vortices are discussed in the online supplementary material available at journals.cambridge.org/flm. Error bars for the meddies are dominated by uncertainties in $(\bar{N}^2 - N_c^2)$, which are due to uncertainties in the reported densities and temperatures of meddies. Meddy Sharon is the oldest meddy shown, so dissipation could have modified its shape.

Based on observations of the haze layers above the GRS and Oval BA, most observers agree that the elevations of their top boundaries (Banfield *et al.* 1988; Fletcher *et al.* 2010; de Pater *et al.* 2010) are near the elevation of 140 mb pressure. Banfield *et al.* (1988) put the top of the upper tropospheric haze that is anomalously elevated over the GRS at 160 mb and the haze over the White Ovals (from which Oval BA formed) at 150 mb. There is less agreement on the elevations of the mid-planes ($z = 0$) of the vortices. Some modellers (Morales-Juberias, Sanchez-Lavega & Dowling 2003) set $z = 0$ to be 680 mb (the height of the clouds from which the velocities are extracted), making $H = 33$ and 34 km, respectively for the GRS and Ovals. However, some observers (de Pater *et al.* 2010) argue that the $z = 0$ planes for both the GRS and the Ovals are deeper at 2000 mb, making $H = 59$ and 60 km for the GRS and Ovals, respectively. Based on these observations and arguments, we set the 'observed' H for both the GRS and the Oval BA to be an average of these values, and we assign to it an uncertainty that is large enough to account for both choices of the elevation of $z = 0$. Thus, we set $H = 46 \pm 14$ km.

Jovian values of $\bar{N}$ have been measured accurately (Shetty & Marcus 2010), and as shown in the online supplementary material, the values of $(\bar{N}^2 - N_c^2)$ and their

uncertainties for the GRS and the Oval BA can be inferred from thermal imaging, which provides the temperatures of the vortices and of the background atmosphere. We show in the online supplementary material how the values and uncertainties of N_c for the GRS and Oval BA that are used in table 1 are calculated from the observed temperature measurements and also how the values of Ro for the Jovian vortices in table 1 were calculated. Using the values in table 1 for the properties of the Jovian vortices and of the background Jovian atmosphere we have included the aspect ratio information of the GRS and Oval BA in figure 4. The figure shows that the aspect ratios of the Jovian anticyclones are consistent with our law (2.4) for α (with the correction due to the fact that $R_v \neq L$ for the GRS). Even with the large uncertainties in H, the data show that the aspect ratios of the Jovian vortices are not equal to $f/\bar{N}$ or to $Ro\,(f/\bar{N})$.

6. Conclusions

We have derived and verified a new law (2.4) for the aspect ratio $\alpha \equiv H/L$ of vortices in stratified, rotating flows; this law depends on the Coriolis parameter f, the Rossby number Ro, the stratification of the ambient fluid $\bar{N}$ and also on the stratification inside the vortex N_c. This law derived in a more general context in the companion paper by Hassanzadeh *et al.* (2012) exactly fits the equilibrium solution of the Boussinesq equations that we used to model our laboratory anticyclones. We have shown that the law works well for predicting the aspect ratios of freely decaying anticyclones in the laboratory, of laboratory vortices that are sustained by continuous fluid injection, of Jovian vortices and of Atlantic meddies. These vortices span a large range of Rossby numbers, occur in different fluids, have different ambient shears, Reynolds numbers and lifetimes, and are created and dissipated by different mechanisms. For these vortices we have demonstrated that a previously proposed scaling law, $H/L = f/\bar{N}$, is not correct. Our law (2.4) for α shows that equilibrium cyclones must have $\bar{N} < N_c$, that anticyclones with $|Ro| < 1$ have $\bar{N} > N_c$ and that anticyclones with $|Ro| > 1$ have $\bar{N} < N_c$. Mixing within a vortex tends to de-stratify the fluid inside of it and therefore naturally decreases N_c from its initial value. Therefore, if there is mixing and if there is no active process that continuously re-stratifies the fluid within a vortex, then at late times one would expect that $N_c < \bar{N}$, and then according to our law only anticyclones with $|Ro| < 1$ can be in equilibrium. This may explain why there are more anticyclonic than cyclonic eddies in the ocean, and also why there appear to be more long-lived anticyclones than cyclones on Jupiter, Saturn and Neptune.

Acknowledgements

We thank the F. B. Fund, Ecole Centrale Marseille and the R. Severance Springer Professorship endowment that permitted this collaborative work. We also acknowledge financial support from the Planetology National Program (INSU, CNRS) and from the NSF AST Program and the NASA Planetary Sciences Program.

Supplementary material is available at journals.cambridge.org/flm.

REFERENCES

ANTIPOV, S. V., NEZLIN, M. V., SNEZHKIN, E. N. & TRUBINIKOV, A. S. 1986 Rossby autosoliton and stationary model of the Jovian Great Red Spot. *Nature* **323**, 238–240.

ARMI, L., HEBERT, D., OAKEY, N., PRICE, J. F., RICHARDSON, P. L., ROSSBY, H. T. & RUDDICK, B. 1988 The history and decay of a Mediterranean salt lens. *Nature* **333**, 649–651.

BANFIELD, D., GIERASCH, P. J., BELL, M., USTINOV, E., INGERSOLL, A. P., VASADA, A. R., WEST, R. A. & BELTON, M. J. S. 1988 Jupiter's cloud structure from Galileo imaging data. *Icarus* **135**, 230–250.

BILLANT, P. & CHOMAZ, J.-M. 2001 Self-similarity of strongly stratified inviscid flows. *Phys. Fluids* **13**, 1645–1651.

BUSH, J. M. W. & WOODS, A. W. 1999 Vortex generation by line plumes in a rotating stratified fluid. *J. Fluid Mech.* **388**, 289–313.

CARTON, X. 2001 Hydrodynamical modeling of oceanic vortices. *Surv. Geophys.* **22**, 179–263.

DRITSCHEL, D. G., DE LA TORRE JUAREZ, M. & AMBAUM, M. H. P. 1999 The three-dimensional vortical nature of atmospheric and oceanic turbulent flows. *Phys. Fluids* **11**, 1512–1520.

FLETCHER, L. N., ORTON, G. S., MOUSIS, O., YANAMANDRA-FISHER, P., PARRISH, P. D., IRWIN, P. G. J., FISHER, B. M., VANZI, L., FUJIYOSHI, T., FUSE, T., SIMON-MILLER, A. A., EDKINS, E., HAYWARD, T. L. & DE BUIZER, J. 2010 Thermal structure and composition of Jupiter's Great Red Spot from high-resolution thermal imaging. *Icarus* **208**, 306–318.

GILL, A. E. 1981 Homogeneous intrusions in a rotating stratified fluid. *J. Fluid Mech.* **103**, 275–295.

GRIFFITHS, R. W. & LINDEN, P. F. 1981 The stability of vortices in a rotating, stratified fluid. *J. Fluid Mech.* **105**, 283–316.

HASSANZADEH, P., MARCUS, P. S. & LE GAL, P. 2012 The universal aspect ratio of vortices in rotating stratified flows: theory and simulation. *J. Fluid Mech.* **706**, 46–57.

HEBERT, D., OAKLEY, N. & RUDDICK, B. 1990 Evolution of a Mediterranean salt lens: scalar properties. *J. Phys. Oceanogr.* **20**, 1468–1483.

HEDSTROM, K. & ARMI, L. 1988 An experimental study of homogeneous lenses in a stratified rotating fluid. *J. Fluid Mech.* **191**, 535–556.

MARCUS, P. S. 1993 Jupiter's Great Red Spot and other vortices. *Annu. Rev. Astron. Astrophys.* **31**, 523–573.

MCWILLIAMS, J. C. 1985 Submesoscale, coherent vortices in the ocean. *Rev. Geophys.* **23**, 165–183.

MEUNIER, P. & LEWEKE, T. 2003 Analysis and treatment of errors due to high gradients in particle image velocimetry. *Exp. Fluids* **35**, 408–421.

MORALES-JUBERIAS, R., SANCHEZ-LAVEGA, A. & DOWLING, T. E. 2003 EPIC simulations of the merger of Jupiter's White Ovals BE and FA: altitude-dependent behavior. *Icarus* **166**, 63–74.

NOF, D. 1981 On the β-induced movement of isolated baroclinic eddies. *J. Phys. Oceanogr.* **11**, 1662–1672.

OSTER, G. 1965 Density gradients. *Sci. Am.* **213**, 70–76.

DE PATER, I., WONG, M. H., MARCUS, P. S., LUSZCZ-COOK, S., ADAMKOVICS, M., CONRAD, A., ASAY-DAVIS, X. & GO, C. 2010 Persistent rings in and around Jupiter's anticyclones: Observations and theory. *Icarus* **210**, 742–762.

PINGREE, R. D. & LE CANN, B. 1993 Structure of a meddy (Bobby 92) southeast of the Azores. *Deep-Sea Res.* (I) **40**, 2077–2103.

REINAUD, J. N., DRITSCHEL, D. G. & KOUDELLA, C. R. 2003 The shape of vortices in quasi-geostrophic turbulence. *J. Fluid Mech.* **474**, 175–192.

SCHLUTZ TOKOS, K. & ROSSBY, T. 1990 Kinematics and dynamics of a Mediterranean salt lens. *J. Phys. Oceanogr.* **21**, 879–892.

SHETTY, S. & MARCUS, P. S. 2010 Changes in Jupiter's Great Red Spot(1979–2006) and Oval BA (2000–2006). *Icarus* **210**, 182–201.

SOMMERIA, J., MEYERS, S. D. & SWINNEY, H. L. 1988 Laboratory simulation of Jupiter's Great Red Spot. *Nature* **331**, 689–693.

TYCHENSKY, A. & CARTON, X. 1998 Hydrological and dynamical characterization of meddies in the Azores region: a paradigm for baroclinic vortex dynamics. *J. Geophys. Res.* **103**, 25061–25079.